ARTICLE IN PRESS

Available online at www.sciencedirect.com

ScienceDirect

International Journal of Rock Mechanics & Mining Sciences ▮ (▮▮▮▮) ▮▮▮–▮▮▮

International Journal of Rock Mechanics and Mining Sciences

www.elsevier.com/locate/ijrmms

Kinematic model for quasi static granular displacements in block caving: Dilatancy effects on drawbody shapes

F. Melo[a], F. Vivanco[a,*], C. Fuentes[b], V. Apablaza[b]

[a]*Departamento de Física Universidad de Santiago de Chile, Center for Interdisciplinary Research in Materials, CIMAT Avenida Ecuador 3493, Casilla 307, Correo 2 Santiago-Chile, Chile*

[b]*Instituto de Innovación en Minería y Metalurgia, IM2 Codelco Avenida del Valle 738, Ciudad Empresarial, Huechuraba, Santiago-Chile, Chile*

Received 1 September 2006; received in revised form 24 May 2007; accepted 2 July 2007

Abstract

A generalized purely kinematic model is proposed for the description of the displacement field in a granular material slowly discharging from a hopper. In addition to the diffusion constant of the well-known kinematic model, our generalized version includes a new parameter accounting for the dilatancy effect that takes place at early stages of the flow. Experimental measurements of particle tracers displacements were made in a ''quasi two-dimensional'' hopper and a promising agreement with the model was found. Applications to quasi static flows occurring in underground mining are discussed. It is shown that the effect of a small dilation on drawbody shapes can be introduced by taking a slightly larger diffusion constant D_P in the kinematic model. As a consequence, the drawbody width W links to the drawbody height H as $W^2 \propto D_P H$, with D_P being a linear function of granulate size. This result that is valid in two and three dimensions, captures the main features of independent laboratory measurements as well as observations performed in operating mines.

PACS: 45.70.Mg; 45.70.Vn; 47.57.Gc

Keywords: Block caving; Isolated extracted zone; Drawpoints; Kinematic flow model

1. Introduction

The prediction of particular type of hopper flows that occur in many underground mines when extracting mineral by the ''block caving method'' [1] is of fundamental importance to optimize ore recovery. The general features of these flows, the related open problems as well as the approaches in use for mining applications have recently been discussed by several authors, for instance, Brown [2] and Rustan [3]. The major difficulty in understanding these flows is the absence of a reliable theory to describe the complex rheological properties of granular materials. In this method, a large number of drawpoints is organized in a periodic lattice such that the geometry and distance between neighbors optimize the global extraction process and ore recovery. To develop insight into the optimization process, experimental efforts have been focused on the prediction of the initial locus of material that is extracted from a single drawpoint. Such a locus is named the ''drawbody'', ''drawzone'' or isolated extracted zone (IEZ) and its size depends mainly on the volume of extracted material. Besides the drawpoints geometry and the distance between them, another important parameter is the average size of granulates which might influence the IEZ size. In addition, even in the case of prefractured procedure, the material inside the cavity is initially in a compact state and dilates as it flows. In turn, the geometry of IEZ provides useful information for the optimization of distance between drawpoints in a mine as well. In practice, the extracted material locus, resulting from either simultaneous or sequential extractions from several drawpoints, is roughly estimated by the elementary geometrical superposition of IEZs produced by drawpoints under study. Although this

*Corresponding author.
E-mail address: fmelo@lauca.usach.cl (F. Melo).

1365-1609/$ - see front matter © 2007 Published by Elsevier Ltd.
doi:10.1016/j.ijrmms.2007.07.005

approximation is rather crude, due to the lack of both analytical models and reliable experimental data, little progress has been made in describing the flow resulting from interactions of several drawpoints. In a recent paper [4], we have briefly reviewed the available models to account for the shape of the IEZ. The Bergmark Roos hypothesis was discussed and it was shown that when the continuity equation is considered, material local density unphysically increases with time. More realistic drawbody shapes were calculated for flows predicted from a plasticity theory model as well as from a kinematic model. Applications to complex configurations where flow is produced by two drawpoints, either in simultaneous or sequential extractions, were discussed in detail. In particular, by taking advantage of the kinematic model's linearity and the geometrical simplicity of the plasticity model, the combined extracted zone was calculated exactly and its dependence on distance between drawpoints was investigated. Here we present several laboratory experiments intended to mimic relevant aspects of flows encountered in copper mining when the block caving technique is applied. Special attention is devoted to the dilation induced by decompaction of the initially compact material. To capture the experimental finding, we derive a simple generalized kinematic model in which local dilation is included in a heuristic constitutive law. In this approximation, the local dilation is assumed to depend only on local grain displacements. A finite elements code is used to solve the model and experiments are performed in a quasi two-dimensional (2D) geometry to check the validity of our assumptions.

2. Gravity flow of broken rocks in caving mines: previous works

In this section, we briefly summarized some attempts to describe the flows of broken rocks taking place in caving mines. This summary is far from being complete since our attention is mainly focused on either laboratory experiments or intermediate scale test that compare, at least partially, with our results. To our knowledge, only a few full scale tests have been carried out to study granular material in caving mines and most of them are for sublevel caving rather than block caving. In our opinion, the available data, although valuable, is not sufficient to provide a detailed description of flows features, hence we do not discuss them here.

Laboratory experiments on sand models are more often developed as scaled systems to mimic underground flows. Kvapil [5,6] attempted first to provide mathematical basis to the granular flow in hoppers and bins. Although simply using a 2D model with colored particles as lines-tracers, this work was extended to idealized large scale flows taking place at iron ore mines and used as a valuable design tool [7]. Based on this model, the shape of both the drawbody zone and the loosening zone were assumed as ellipsoidal. One of the important results of this study is that, the volume of discharged material, Ω, links to the draw ellipsoid height H and width W as, $W/2 = \sqrt{\Omega/(2.094H)}$. In addition, scale factors between both ellipsoids were proposed, for instance, the width of loosening zone W_1 scaled as $W_1 \approx 2.5W$.

Several authors including Heslop, Laubscher, and Marano [8–11] developed experiments in a 3D model to investigate the interactive drawing of adjacent drawpoints. The laboratory container had 76 cm long, 76 cm wide and 240 cm height, whose base contained 50 drawpoints of 2.5 cm in diameter, evenly spaced. The spacing between drawpoints could be varied for different experimental conditions. Care was taken to simulate the actual geometrical condition in mines. The material used was sand, with average size of 0.7 mm. Drawpoints in this model were drawn simultaneously and the movement of the material under draw was followed by the help of colored layers of sand. At the end of representative runs, water was poured on top of the sand model, in order to wet it homogeneously. Wet sand provided enough cohesion to allow the cutting of vertical sections through the material, revealing the position of the colored layers.

The same authors carried out experiments in which the drawpoints were spaced at the width of a previously measured isolated drawzone (IEZ). A uniform lowering of the upper markers occurred when the drawpoints were drawn simultaneously. This result was then compared to the reconstructed drawzone of isolated drawpoint experiment, concluding that the ellipsoid theory does not apply in this situation. According to our previous work [4], in which we describe in some detail how the interacting flows can be treated in a linear approximation, both situations are not equivalent and therefore different tracers motion are expected.

Laubscher [9,10] then proposed a phenomenological flow interaction theory, stating that optimal interaction will occur when the drawpoints are spaced at 1.5 times the width of the isolated drawzone. Although this criterium is of intensive practical use when optimizing block caving mines, a detailed analysis of drawpoints interaction is still lacking. Our linear theory of flow interactions presented in Section 5.3 provides a mathematical support to this type of criterium.

Model experiments using gravel instead of sand at relatively large scale [12–14] have been developed providing both useful and apparently contradictory information on *IEZ*s geometry. For instance, in Peters' model [13], where an essentially 2D system with broken rock, sized at 0.5, 1.0, and 1.5 in along with the equal fraction mixtures of these sizes have been used, it is shown that the resultant width of the draw envelope is not affected by the particle size. This result seems to contradict Kvapil's ellipsoid theory. In turn, Power [14] carried out tests in a 3D gravel model and did find a small particle size effect on the width of the draw envelope. It is worth to note that our calculations based on kinematic model [4] predicts that $W \propto d^{1/4}$, which is compatible with Power results if d is taken as the average

Please cite this article as: Melo F, et al. Kinematic model for quasi static granular displacements in block caving: Dilatancy effects on drawbody.... Int J Rock Mech Mining Sci (2007), doi:10.1016/j.ijrmms.2007.07.005

particle size. In addition, for 2D system, we predicts [4], $W \propto d^{1/3}$, which is still a slowly varying function of d and might explain why Peters did not observe appreciable variation of W. In our opinion, data reported in Ref. [13] are compatible with $\frac{1}{3}$ power law if the width of the drawpoint is included properly, see Section 5.2.

3. Granular flow: kinematic model

Despite its complexity, the flow of granular materials can be described by hydrodynamical models whenever all the relevant characteristic dimensions of the container are much larger than granulate size. This approximation has been supported by experimental studies conducted by ourselves and many others, see for example [15], considering different particle shapes, irregular and spherical and even mixtures [16]. Thus, we expect that not only laboratory experiments fulfill the requirement for hydrodynamical approximation but, many flows taking place during underground mining when granulated material of narrow size distribution is involved. To our knowledge this condition is at least fulfill partially or temporally in many operating mines. Several effects might, however, challenge the prediction capability of hydrodynamical approach when applied to mining, for instance, the presence of relatively large inhomogeneities in granulate size and material properties, the size reduction due to friction and high pressure, as well as large fluctuations due to jamming or shear bands [17]. Detailed descriptions of these situations, suitable for practical applications, have not been developed until present.

Typical candidates amenable to be treated by hydrodynamical approaches are the granular flows driven by gravity found in hoppers. In this approximation two distinct regimes can be found, namely viscous and inertial. The former regime develops when gravity is balanced by an effective viscosity. However, since Bagnold it is well accepted that no intrinsic viscosity exists in granular materials as in diluted gases. As was suggested by Bagnold [18], the viscous stress σ is a quadratic function of both the local shear rate $\partial_x V$, and the particle diameter d, i.e., $\sigma \sim d^2(\partial_x V)^2$. Then, when gravitational acceleration, g, is included the Bagnold law for the mean flow, $V \sim \sqrt{gR^3}/d$, is obtained. This law is not only a function of the hopper aperture R, but also of the granulate size d. To our knowledge there is no experimental evidence to support this regime. On the other hand, when gravity balances inertia, i.e., the usual convective term in transport equations, we obtain the inertial regime in which the typical mean speed, $V \sim \sqrt{gR}$, is independent of the grain size. This regime is well observed experimentally in a wide variety of granular materials [19,20]. Note that in a simple fluid, the characteristic length scale is the fluid level H, and the mean velocity is given by $V \sim \sqrt{gH}$. Many theoretical models have been developed to explain this deep difference between granular materials and fluids. A more elaborate approach to predict velocity distributions of granular materials is based on plasticity theory [17], where the velocity distribution is obtained from the stress distribution calculated in the static material. In spite of the apparent simplicity of these models, little progress has been made in predicting velocity fields in complex configurations. To overcome these difficulties, several authors proposed alternative approaches by either modeling the flow as the upward diffusion of voids [21] or by considering the probability of granulate motion as a random process [22]. In both cases, the velocity diffuses upward from the aperture. Following the same ideas, Nedderman and Tüzün [23], developed a model in which the particles located immediately above the orifice fall down, letting the particles in the upper layers slide into the vacant space. Thus, it is expected that the horizontal velocity depends on the gradient of the vertical velocity, $U = -D_p \partial_x V$. Using mass conservation, it is easily found that $\partial_y V = D_P \partial_{xx} V$. The same authors have shown that the kinematic model is successful in describing the velocity distribution in a rectangular hopper under stationary conditions, when the material is in a loose packing state [23]. However, if the material inside the hopper is in a nearly compact state the agreement becomes poor [24], due to the dilation that takes place when a densely packed granular material starts to flow. Recent experimental results [16,25] confirm these findings and show that streamlines are correctly predicted by kinematic models in the loose packing regime.

4. Experimental results

Our experimental setup is described in detail in Ref. [26]. Here we discuss a few aspects necessary to contrast experimental finding with the theoretical models developed below. A quasi 2D flat bottomed hopper was designed to observe the flow of grains, Fig. 1. This hopper is made of

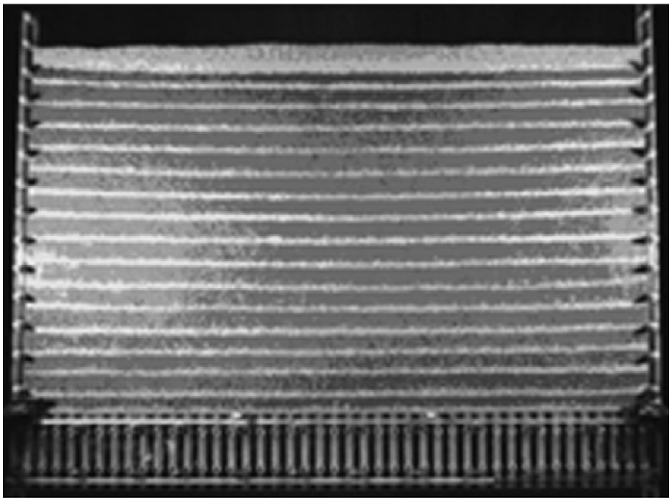

Fig. 1. Front view of the experimental set up. Horizontal lines, 3 cm apart, are made of colored particles used as tracers. A network of equidistant apertures, 2 cm apart, allows to explore flow interactions for a wide range of aperture distances.

Please cite this article as: Melo F, et al. Kinematic model for quasi static granular displacements in block caving: Dilatancy effects on drawbody.... Int J Rock Mech Mining Sci (2007), doi:10.1016/j.ijrmms.2007.07.005

two parallel plexiglass plates, with 110 cm wide and 100 cm height, held a distance $h = 2$ cm apart by a rigid frame. The space between the plates was filled with glass beads of $d = 2$ mm diameter at some intermediate packing. To characterize the motion of the grains horizontal lines of colored material were located equally spaced. These lines are labeled by their vertical positions, $y_m = m\Delta y$, where m is an integer and $\Delta y = 3$ cm, see Fig. 1. The vertical deflection of the lines corresponding to the particle displacements was recorded each time a certain amount of material was extracted. To extract material from the hopper several equidistant cylindrical holes were drilled centered and perpendicular to its base. The holes located 2 cm apart are 1 cm in diameter and 7 cm in length. Every cylindrical aperture is also provided with a flush mounted valve located at the upper end, allowing us to select configurations with different active hopper apertures. This setup provides a simple way to investigate configurations where the flow is produced by a single aperture or multiple apertures. In order to study the interaction of flows, the distance between adjacent active holes is considered a variable. More complex situations are possible to obtain and are reported elsewhere. An extra valve is located at 4.5 cm below the upper valve of each cylindrical hole allowing for precise control of the extracted volume. It is aimed to mimic the actual discrete process during the extraction of material taking place in the mine. Fig. 2 illustrates the tracers' motion after one, three and five volume extractions, respectively. The deflection of tracer lines decreases until vanishing at long distance from the aperture. Useful information can be obtained by defining the locus of granulates that moves a distance larger than an arbitrary value after an extraction of material is done.

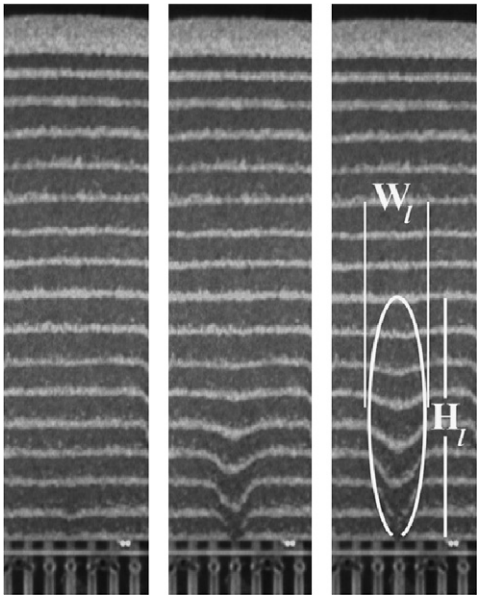

Fig. 2. Front view. Tracer lines deflection produced by granulate displacement from a single drawpoint for one, three and five extractions, respectively. Solid line on the right panel represents the loosening region of maximum width W_1 and height H_1.

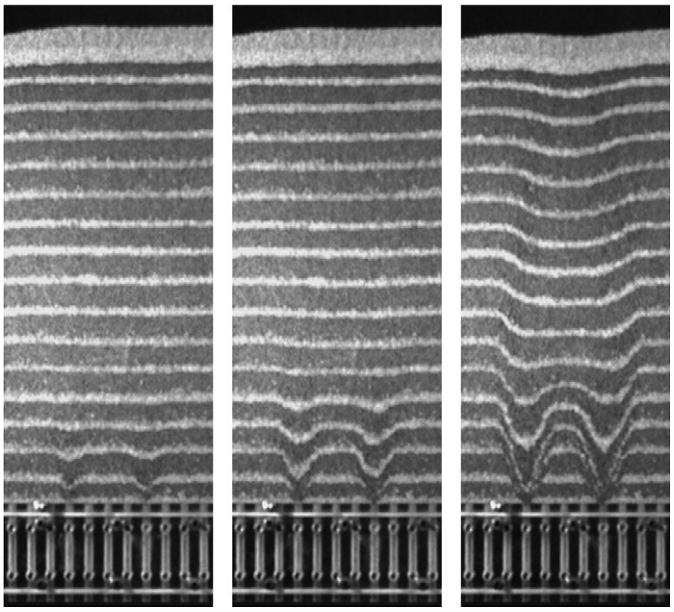

Fig. 3. Tracer lines deflection produced by granulates displacements in the case of two apertures in simultaneous extractions. The distance between drawpoints is 8 cm. Left panel: after two extractions. Middle panel: after four extractions. Right panel: after eight extractions.

This locus is named "loosening region", and its extension depends on the criterium used to determine whether or not the granulates substantially move. In our experiments, the loosening region includes all the granulates displaced more than a fraction of a granulate diameter, and its width W_1 increases with the extracted section S roughly as $W_1 \sim S^{0.5}$ [26]. Notice that in our quasi 2D model the extracted volume Ω can be written as, $\Omega = hS$.

Displacement of the tracer lines, in the case of flows created by two drawpoints in simultaneous extraction, are illustrated in Fig. 3. The interaction of flows is not observed in the regions located very close to the aperture, the granulate motion seems to be similar to the isolated hoppers, see Fig. 2. However, such interaction becomes visible quickly with increasing vertical distance from the aperture. Remarkably, in the central region, the tracer lines move downwards while remaining horizontal, with small lateral deformations, as would occur in a constant descending flow. The main features of this combined flow can be captured by the linear superposition of isolated flows. This is discussed in more detail using the kinematic model framework in the next sections.

5. Two-dimensional flows

Both, the experiments described above and the hopper flows occurring in underground mines when the block caving method is applied, can be considered, in a first approximation, as a quasi static process. In the caving method, for instance, it is very often that the flux of granulate is limited by the frequency of material extraction; a given mass of material is taken from the drawpoint and

Please cite this article as: Melo F, et al. Kinematic model for quasi static granular displacements in block caving: Dilatancy effects on drawbody.... Int J Rock Mech Mining Sci (2007), doi:10.1016/j.ijrmms.2007.07.005

then the granular column is allowed to relax until a new extraction is required. In such situations, the average granulate speed at the aperture is clearly restricted by the speed of the extraction operation which is relatively slow compared to the free flow. For a discrete extraction process, the time scale is irrelevant and the granulate displacement, imposed at the drawpoint, is more relevant than the granulate speed. Thus, the kinematic model writes,

$$u = -D_P \frac{\partial v}{\partial x}, \tag{1}$$

where u and v are the horizontal and vertical displacements of granulate, respectively. In addition, if the material is initially in a compact state, at every extraction some irreversible dilation takes place. The equation above neglects any volume increases induced by the local dilation. This effect will be included later in the text. Using the continuity equation and ignoring dilation,

$$\frac{\partial u}{\partial x} + \frac{\partial v}{\partial y} = 0, \tag{2}$$

a diffusion equation can be obtained for the vertical evolution of an imposed vertical displacement at the aperture. This is,

$$\frac{\partial v}{\partial y} = D_P \frac{\partial^2 v}{\partial x^2}, \tag{3}$$

which can be solved for given boundary conditions at the aperture or drawpoint.

5.1. Single aperture

Let us begin studying the case of a single aperture of finite size in a flat bottomed hopper, such that the boundary conditions are specified at the aperture only. Orienting the reference frame in such a way that it is centered at the aperture of width $2R$, the boundary conditions at $y = 0$ are, $v = -v_0$ for $-R < x < R$, and $v = 0$ for $x < -R$ and $x > R$. With these conditions, the solution of the diffusion equation is a superposition of two error functions,

$$v(x,y) = -\frac{v_0}{2}\left[erf\left(\frac{x+R}{\sqrt{4D_P y}}\right) - erf\left(\frac{x-R}{\sqrt{4D_P y}}\right)\right]. \tag{4}$$

In turn, the calculation of the horizontal displacement u can be easily obtained from Eq. (1). It reads,

$$u(x,y) = -\sqrt{\frac{v_0^2 D_P}{4\pi y}}\left[e^{-(x+R)^2/4D_P y} - e^{-(x-R)^2/4D_P y}\right]. \tag{5}$$

Instead of plotting the whole displacement field, we follow the motion of marked particles, located initially in a network of equidistant horizontal lines 3 cm apart along the vertical, and labeled by the vertical coordinate y_m, i.e., $y_m = m\Delta y$, with $\Delta y = 3$ cm, as in the experiments, see Fig 1. In practice to perform the calculations, it is necessary to impose a displacement at the aperture, named here "step" v_0, smaller than the particle diameter, $v_0 \leqslant d$. Then, the new positions of the dyed particles are calculated. To observe the evolution of the system at the end of an actual single extraction, as many "steps" as necessary are executed until completing the "section" of one extraction, S. If a similar displacement is imposed at each step, then the displacement field does not need to be recalculated. However, in a Lagrangian description, the step process is required to accurately calculate the new positions of marked particles. When these results, shown in Fig. 4, are contrasted to the experimental results, see Fig. 2, we observe an interesting qualitative agreement between the tracers displacement in locations near to the aperture. In Fig. 4 the coefficient, D_P, is taken equal to the granulate size. This is justified later in the text. However, it is observed experimentally that granulate displacements at the drawpoint do not affect regions located far from the aperture. This difference between experiment and model is due to the assumption of constant density. In other words, the kinematic model preserves the area explored by the tracer lines since any displacement at the aperture diffuses along the vertical. This discrepancy can be reduced by

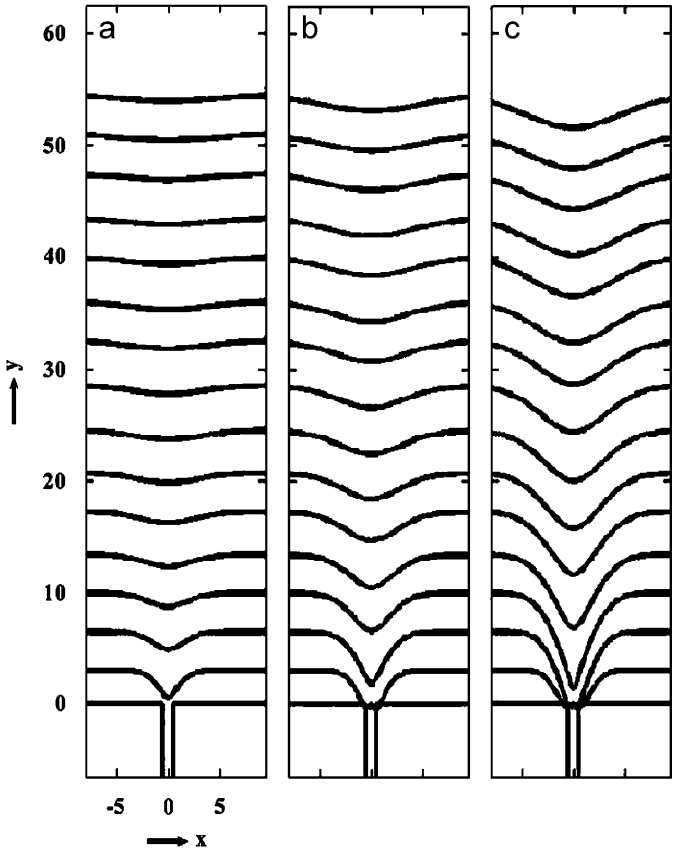

Fig. 4. Calculations of particles displacement at several vertical levels, for a diffusion coefficient $D_P = d$. Here $v_0 = d$, with $d = 0.2$ cm, $2R = 1$ cm, and a single extraction corresponds to a section of removed material, $S = 4.5\,\text{cm}^2$. (a) Particles displacement after one extraction; (b) particles displacement after three extractions; (c) particles displacement after five extractions.

Please cite this article as: Melo F, et al. Kinematic model for quasi static granular displacements in block caving: Dilatancy effects on drawbody.... Int J Rock Mech Mining Sci (2007), doi:10.1016/j.ijrmms.2007.07.005

introducing the density variations through the concept of dilation by decompaction as it is shown in Section 7.

5.2. Drawbody shapes

A few well-known concepts, such as stream lines, drawbody shapes and motion zone can be revisited from the point of view of the above simple description. In the 2D flow, the streamlines are parallel to the displacement of the particles and, therefore, they obey the following equation:

$$\frac{\mathrm{d}x}{u} = \frac{\mathrm{d}y}{v}. \tag{6}$$

For the case of a narrow aperture, the above equation can be integrated analytically and the IEZ calculated exactly [4]. However, for finite size apertures, an analytical solution of Eq. (6) is difficult to obtain. We then integrate it numerically by a simple shooting method. Left panel in Fig. 5 shows that the streamlines are nearly parabolas at regions far from the hopper aperture. However, near the symmetry axis of the aperture and at vertical distances of the order of its size, the streamlines are nearly parallel. In the usual definition, a drawbody is the geometrical initial location of the particles that, after one extraction, cross the aperture. Equivalently, a drawbody is simply the surface demarcating the zone of material to be extracted. Left panel in Fig. 5 includes the IEZ for increasing amount of extracted material. Near the aperture, the lateral diffusion of the vertical displacement is dominant and the IEZ wider. For a full discussion on drawbody shapes resulting from different types of granular flows see Ref. [4]. Here let us recall that for narrow apertures in two dimensions, the IEZ height H is linked to the width W as, $W^2 = (24/e)D_{\mathrm{P}}H$. In the case of finite aperture of size $2R$, this result holds for a large amount of extracted material. However, at early stages of extraction the aperture size dominates. Right panels in Fig. 5 show how the dimensions of IEZs, obtained for a finite size aperture, deviate from the shape calculated for extremely narrow aperture [4]. For this latter, $H \propto S^{1/3}$, $W \propto S^{2/3}$ and $W \propto \sqrt{H}$.

5.3. Flow interactions: two apertures in simultaneous extraction

We now discuss the flows produced by two apertures located at a certain distance apart. In the framework of the kinematic model, which is a linear approximation, the flow due to several apertures simply corresponds to the superposition of the flow produced by individual apertures. In general, this is written as

$$\vec{v} = \sum_{\vec{L}_i} \vec{v}_{v_{0i}}(\vec{x} - \vec{L}_i), \tag{7}$$

where $\vec{v}_{v_{0i}}$ is the displacement field produced by a single aperture with vertical displacement $\vec{v}_{0i}$ at the hopper aperture centered at position $\vec{L}_i$. In other words, the knowledge of the flow produced by a single aperture makes it possible to construct the flow of multiple drawpoints, when the extraction takes place simultaneously.

For simplicity, we calculate the trajectory lines and drawbody shape in the case of two apertures of finite width, separated by a given distance, and within the kinematic approximation. As stated above, the velocity field is the superposition of the two contributions. Then, for apertures of width $2R$, located symmetrically on the horizontal axis, and separated a distance $2L$, the vertical

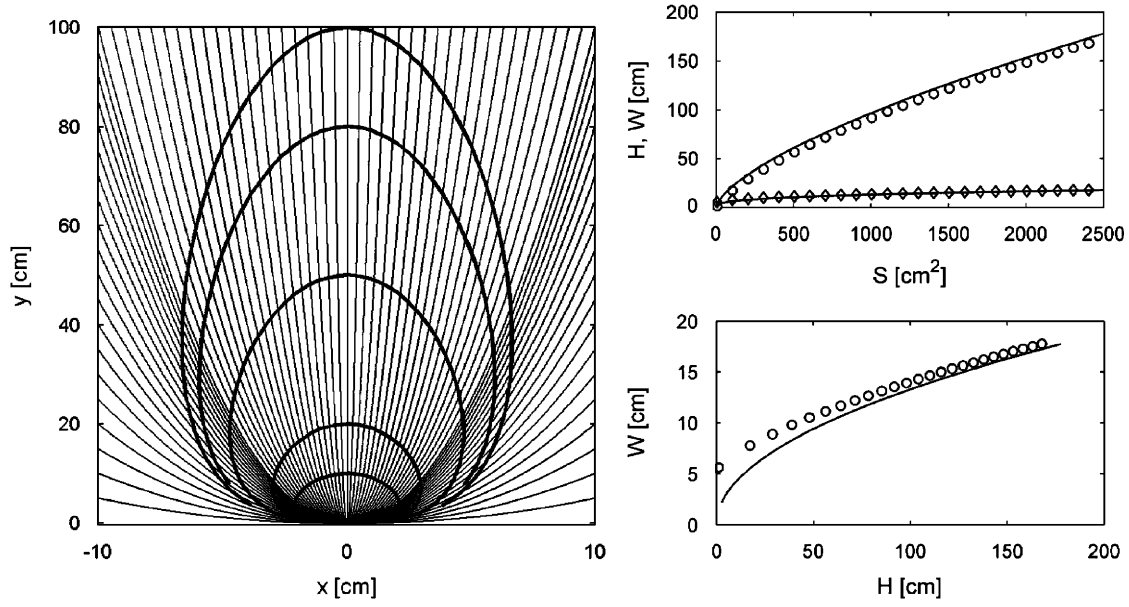

Fig. 5. Left panel: thinner lines are the trajectories of particles in the kinematic model description, for $D_{\mathrm{P}} = d$, $R = (5/2)d$ and $d = 0.2$ cm. Thicker lines are the drawbodies shapes for increasing extracted section S of material, namely, $S = 17, 48, 190, 380, 530\,\mathrm{cm}^2$. Right panels: open symbols stand for calculated features H (rhombus) and W (circles) of IEZs, for the finite size aperture case, whereas solid lines are the power laws obtained in Ref. [4] for extremely narrow aperture.

Please cite this article as: Melo F, et al. Kinematic model for quasi static granular displacements in block caving: Dilatancy effects on drawbody.... Int J Rock Mech Mining Sci (2007), doi:10.1016/j.ijrmms.2007.07.005

displacement reads,

$$v(x,y) = -\frac{v_0}{2}\left[erf\left(\frac{x-L+R}{\sqrt{4D_P y}}\right) - erf\left(\frac{x-L-R}{\sqrt{4D_P y}}\right)\right] - \frac{v_0}{2}\left[erf\left(\frac{x+L+R}{\sqrt{4D_P y}}\right) - erf\left(\frac{x+L-R}{\sqrt{4D_P y}}\right)\right]. \quad (8)$$

The respective horizontal displacement u, after an elementary extraction, can be easily obtained from $u = -D_P(\partial v/\partial x)$. Thus, with the help of the above considerations, the total displacement is evaluated numerically to follow the deflection of tracer lines. The calculations of such deflections are presented in Fig. 6 for several amounts of extracted granular material. The interaction zone is clearly visualized in the region between the two apertures, specially far above the apertures where the displacement of tracer lines might become nearly parallel. It can be easily anticipated that, if the diffusion coefficient D_P is small and apertures are too far apart, the flows due to single apertures may not interact. A detailed discussion of the criterium and parameters that determine whether or not interaction of flows occurs is given in Ref. [4].

The streamlines and drawbody shapes for double aperture hoppers are calculated numerically and presented in Fig. 7 for increasing amount of extracted material. The flow interaction is well visualized between the two apertures where streamlines are nearly parallel. On the other hand, far from the apertures and outside of the middle region, the streamlines are parabolas whose curvature is solely determined by the diffusion coefficient.

6. Three-dimensional flows

In order to compare the kinematic model's predictions with the experimental results, we will solve this model in three dimensions and take into account the exact geometry employed in the experiments. With the assumption of a constant diffusion coefficient, the kinematic model is generalized to three dimensions as

$$u = -D_P\frac{\partial v}{\partial x}, \quad (9)$$

$$w = -D_P\frac{\partial v}{\partial z}. \quad (10)$$

By including these expressions into the continuity equation and neglecting the density variations, the equation for the vertical displacement v, can be written as

$$\frac{\partial v}{\partial y} = D_P\left[\frac{\partial^2 v}{\partial x^2} + \frac{\partial^2 v}{\partial z^2}\right]. \quad (11)$$

Now, the geometry of the system and a set of boundary conditions must be provided to determine the displacement field. Let us consider a Cartesian coordinate system centered at the bottom of the box, such that the system is extended from $-L_x$ to L_x, 0 to L_y and $-L_z$ to L_z in the x, y and z directions, respectively. A rectangular hole is located centered at the base of the box and it is defined such that, $-D_x \leqslant x \leqslant D_x$ and $-D_z \leqslant z \leqslant D_z$, where $D_x < L_x$ and $D_z < L_z$. On the other hand, the boundary condition in the vertical direction is related to the extraction procedure at the hopper aperture. While the lateral boundary conditions, restricting the horizontal movement of the material to inside the box, are given by $u|_{\pm L_x} = \partial v/\partial x|_{\pm L_x} = 0$ and $w|_{\pm L_z} = \partial v/\partial z|_{\pm L_z} = 0$. In order to reproduce the actual experimental situation the displacements are calculated at the front wall of the hopper, where the colored tracer particles are visible in the experiment, i.e., $v(x, y = m\Delta y, z = +L_z)$. Notice that, the experimental

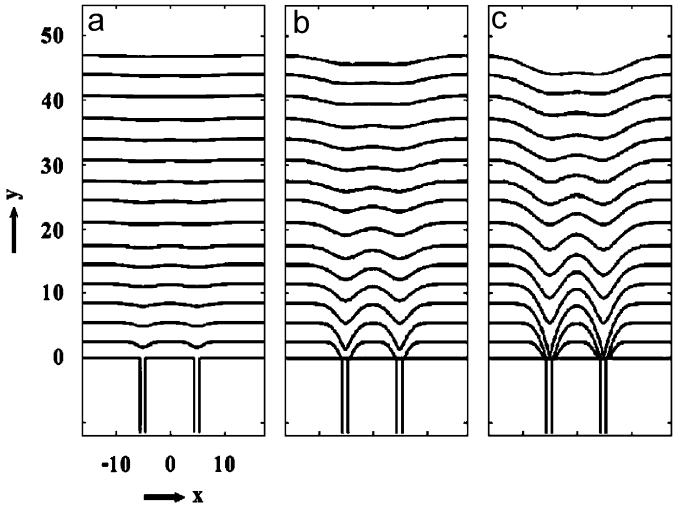

Fig. 6. Snapshots of particles displacement at several levels, for two apertures 8 cm apart. The size aperture is $2R = 1$ cm and the diffusion coefficient is $D_P = d = 0.2$ cm. As above, a single extraction, at a given aperture, corresponds to $S = 4.5\,cm^2$. Here $v_0 = d$. (a) Particles displacement after one extraction; (b) particles displacement after three extractions; (c) particles displacement after five extractions.

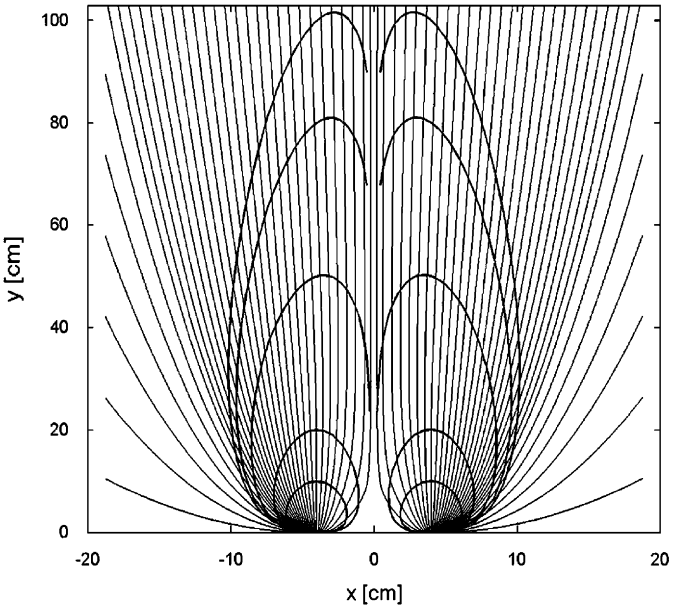

Fig. 7. Draw body resulting from the interaction of the flow produced by two apertures for increasing extracted section $S = 40, 190, 350, 630, 830\,cm^2$. The parameters are $D_P = d$, $R = (5/2)d$, $L = 40d$, $d = 0.2$ cm.

flow is 3D even though the hopper gap $2L_z$ is small compared to the other lengths. The linear nature of the Eq. (11) allows to use the separation of variables method, then we can write $v = X(x)Y(y)Z(z)$. Replacing v into Eq. (11) and introducing the separation constants k_x and k_z the following three equations are obtained, $\partial^2 X(x)/\partial x^2 + k_x^2 X(x) = 0$, $\partial^2 Z(z)/\partial z^2 + k_z^2 Z(z) = 0$ and $\partial Y(y)/\partial y + D_P[k_x^2 + k_z^2]Y(y) = 0$. The first two equations admit a linear combination of harmonic functions as a solution, i.e., $A_x \cos x + B_x \sin x$ and $A_z \cos z + B_z \sin z$, while the solution of last equation can be written as $Y(y) = E \exp -[k_z^2 + k_x^2]D_P y$. The symmetry requirements imply that $B = D = 0$. On the other hand, the separation constants are determined by imposing the lateral boundary conditions and are given by $k_x = (m\pi/L_x)$ and $k_x = (n\pi/L_z)$, where $m, n = 0 \cdots \infty$. Finally, the vertical displacement is given by the linear combination of the solutions characterized by the numbers m and n, that is $v = \sum_{n,m=0}^{\infty,\infty} A_{nm} \cos(n\pi/L_x x) \cos(m\pi/L_z z) \exp(-D_P[(n\pi/L_x)^2 + (m\pi/L_z)^2]y)$, where the constants A, C and E were refunded in the coefficients A_{mn}. These coefficients depend on the vertical boundary conditions which is related to the material extraction process. As an example, let us consider a boundary condition given by a constant volume of extraction, i.e., $v(x, y = 0, z) = -v_0$, then the coefficients that characterize the vertical displacement are given by $A_{mn} = -v_0(4/\pi^2 mn) \sin(m\pi D_x/L_x) \sin(n\pi D_z/L_z)$. Replacing v in Eqs. (9) and (10) the lateral displacements can be determined. In Fig. 8, it is shown the vertical displacements after one and three extractions, respectively. Using D_P as an adjustable parameter, good agreement is obtained for the particles located near to the aperture if D_P is close to d. However, theoretical predictions become gradually poorer for particles located at higher vertical positions. It is worthy to note that, due to the constant density hypothesis involved in the calculations, the integrated deflection, for all initially dyed horizontal lines, must be basically the total section of granulate extracted from the aperture. This condition is clearly not fulfilled for the experimental deflections. Therefore, dilatancy effects must be taken into account. For the double aperture case, the displacement field can be directly calculated by the superposition of the contributions from each aperture. Comparisons—not presented here—of these results with experimental ones provide a good agreement near the aperture. However, similar to the results presented in Fig. 8, far above the apertures, the agreement becomes poor due to dilation effects.

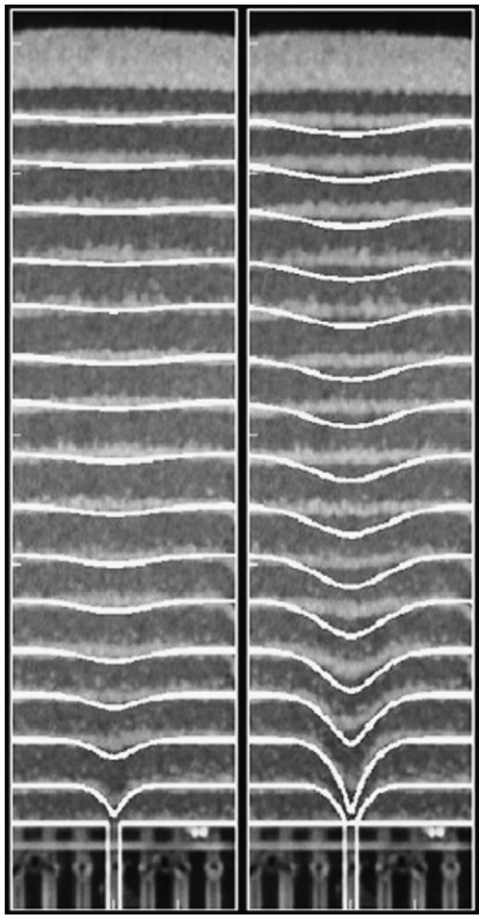

Fig. 8. Granulates displacement at several height levels, as observed experimentally, compared to calculations in three dimensions, for $D_P = d$ and the exact geometry of the experiment. Left panel: after one extraction. Right panel: after three extractions.

7. Dilatancy effects

Although it seems quite natural to assume that the dilation effect is the main reason for the partial disagreement between the experimental and theoretical displacement fields, we provide some more evidence to support this assumption by exploring the amount of light transmitted through the granular material when the number of extractions is increased. The snapshots depicted in Fig. 9 were taken while illuminating the granulate from behind homogeneously. Thus, the small packing variations are detected by contrast difference on the picture. Naturally, the observed increase of light transmission is due to some dilation which in turn is produced by granulate motion. Panels of Fig. 9 also give useful indications of the boundaries of motion-loosening-zone.

For simplicity, we investigate dilatancy effects in 2D configurations. Notice that for the experiments presented here, this approximation holds since the dilation effects are significant only far from the aperture, where our configuration can be considered as truly 2D. One evidence of this fact is that the profile of the free surface does not vary along the axis perpendicular to the parallel walls, see Fig. 9. One possible way to account for dilation in the kinematic model is by means of introducing the additional displacement $u_\delta(v)$ and $v_\delta(v)$, due to local packing variation, such that Eq. (1) becomes,

$$u = -D_P \frac{\partial v}{\partial x} + u_\delta(v), \tag{12}$$

Please cite this article as: Melo F, et al. Kinematic model for quasi static granular displacements in block caving: Dilatancy effects on drawbody.... Int J Rock Mech Mining Sci (2007), doi:10.1016/j.ijrmms.2007.07.005

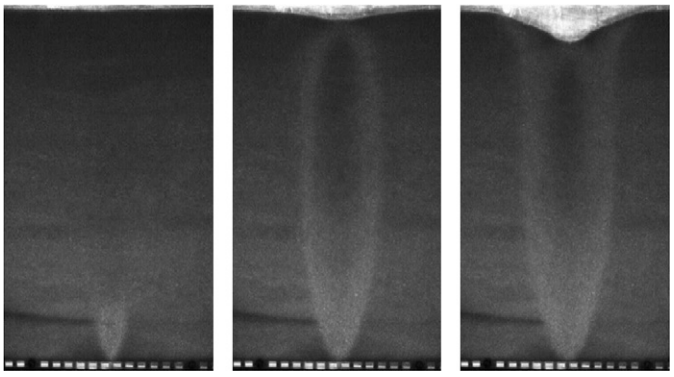

Fig. 9. All panels are front views of the granular compact as produced when intense transmitted light is used. Zones of lower densities appear more illuminated and correspond to regions in which granulate displacement took place.

where $u_\delta(v)$ is an implicit function of space through the vertical displacement v. Then, the continuity equation reads,

$$\delta\rho + \rho\vec{\nabla}\cdot\vec{v} + \vec{v}\cdot\vec{\nabla}\rho = 0, \tag{13}$$

where we will assume that the advection of density gradients, $\vec{v}\cdot\vec{\nabla}\rho \sim 0$, is small, since the density variation is mainly induced when a density front moves upwards. In this case Eq. (13) becomes,

$$\frac{\partial u}{\partial x} + \frac{\partial v}{\partial y} = \Delta S/S_0 = \left[\frac{\partial u_\delta(v)}{\partial x} + \frac{\partial v_\delta(v)}{\partial y}\right], \tag{14}$$

where $\Delta S/S_0$ is the relative variation of the section occupied by the material. Differentiating Eq. (12) and with the help of Eq. (14), it is found that,

$$\frac{\partial v}{\partial y} = D_P\frac{\partial^2 v}{\partial x^2} + \frac{\partial v_\delta(v)}{\partial y}, \tag{15}$$

and

$$\frac{\partial u}{\partial x} = -D_P\frac{\partial^2 v}{\partial x^2} + \frac{\partial u_\delta(v)}{\partial x}, \tag{16}$$

in which dilatancy terms are unknown and difficult to derive from first principles. Therefore, we will look for suitable heuristic approximations for these quantities.

Let us first consider an ideal case in which diffusion is turned off and a small displacement is imposed at the hopper aperture, whose size is taken to be much larger than the average granulate diameter. Then, take dilatancy as a function of the local displacement only. If we assume that the entire granulate is initially in a homogeneous state of a given packing, for instance a random close packing (RCP), and after some motion of grains $|v| \gg d$, it dilates to a random loose packing (RLP), such a function must saturate to a maximum dilation value α_0, which is simply the relative difference between the initial and final packing, in this case, $\alpha_0 = \alpha_{rcp-rlp}$. However, when the displacement is small, i.e., $|v| \ll d$, the dilation should vanishes. The simplest choice that satisfies the above requirements reads,

$$\frac{\partial v}{\partial y} = -\alpha_0 \tanh\frac{v}{d}, \tag{17}$$

which in the limit of small displacement becomes,

$$\frac{\partial v}{\partial y} = -\alpha_0\frac{v}{d}, \tag{18}$$

that predicts an exponential decrease of the vertical displacement as a function of height.

To handle compressions, that in our configuration would occur when imposing positive displacements at the hopper aperture, α_0 needs to be replaced by its respective value. For instance, the one characterizing a transition from RLP to a more compact state. Note that α_0 is defined here as positive.

At this stage, we justify in more detail the approximations involved in deriving Eq. (18). Although it has been well known since Bagnold's time that shear induces dilation, in our case, we have assumed that the main mechanism of dilation is decompaction instead of shear. Simple scale arguments allow us to sustain such an assumption. The two main contributions to dilation induced by shear are estimated to be: $\partial u_\delta/\partial x_{shear} \sim \alpha_0(\partial v/\partial x)$, and $\partial v_\delta/\partial y_{shear} \sim \alpha_0(\partial u/\partial y)$. Where the terms at the right indicate that a dilation of a fraction α_0 occurs when the particles experience a shear of order 1, or equivalently, when the granulates under scope glide a distance of one diameter over their nearest neighbors.

Using the kinematic model and mass conservation, these expressions can be rewritten as, $\partial u_\delta/\partial x_{shear} \sim (\alpha_0/D_P)u \sim (\alpha_0 v_0/\sqrt{D_P y})$ and, $(\partial v_\delta/\partial y_{shear}) \sim \alpha_0 D_P(\partial^2 v/\partial y\partial x) \sim (\alpha_0 v_0/\sqrt{D_P y})(D_P/y)$, where v_0 is the scale of vertical displacement. Since in our coarse grained approximation the vertical coordinate is always larger than the particle diameter, $y \gg d$, $\partial u_\delta/\partial x_{shear} \gg \partial v_\delta/\partial y_{shear}$. Now the decompaction contribution to dilation becomes, $\partial v_\delta/\partial y \sim (\alpha_0/d)v \sim (\alpha_0/d)v_0$, which clearly dominates over the shear contribution. Notice that dilation cannot take place indefinitely and must cease once the granulate has reached the loosest state. This effect is not important for the rough estimate above. Thus, in the following, we only consider the decompaction contribution to dilation as given by Eq. (18) and $\partial u_\delta/\partial x \sim 0$.

7.1. Diffusion dilation equations

Coming back to our original problem, we write the equation for the displacement field including diffusion as well as dilation. When $|v| \ll d$, it reads,

$$\frac{\partial v}{\partial y} = D_P\frac{\partial^2 v}{\partial x^2} - \alpha_0\frac{v}{d}. \tag{19}$$

The small displacement approximation is preferred instead of Eq. (17) to follow more precisely the trajectories of the tracer particles. Indeed, to mimic a single extraction, we produce successive small displacements of equal size,

labeled by the index n, at the hopper aperture until removing the desired amount of material. Thus, for every step, the displacement field is obtained and the new tracer positions are calculated accurately. Another advantage of the small displacement approximation is that the local density of the material can be refreshed at each step, producing more realistic results. In summary, the generalized diffusion dilation equation for step n, can be written as

$$\frac{\partial v^n}{\partial y} = D_{\mathrm{RLP}} \frac{\partial^2 v^n}{\partial x^2} - \Delta D f(v_{\mathrm{T}}/d) \frac{\partial^2 v^n}{\partial x^2} - \alpha_0 f(v_{\mathrm{T}}/d) \frac{v^n}{d}, \qquad (20)$$

where v^n is the displacement field produced by the step n and $v_{\mathrm{T}} = \sum_{i=0}^{n-1} v^k$ is the total local-displacement ($v_{\mathrm{T}} = v_{\mathrm{T}}(x, y)$) after $n-1$ steps. The function $f(v_{\mathrm{T}}/d)$ insures that the local dilation is reduced with the cumulated local displacements, in such a way that dilation vanishes when the total displacement v_{T} is larger than d. In short, $f(v_{\mathrm{T}}/d)$ is taken as $\mathrm{e}^{-|v_{\mathrm{T}}|/d}$ which assures that the system stops dilating after a set number of steps. In addition, it can be seen that the diffusion coefficient D_{P} is now defined as, $D_{\mathrm{RLP}} - \Delta D \mathrm{e}^{-|v_{\mathrm{T}}|/d}$, which includes the variation of D_{P}, ΔD, due to the dilation occurring when the material dilates from the RCP to the RLP state. D_{RLP} is the diffusion coefficient for a RLP state, $\Delta D = D_{\mathrm{RLP}} - D_{\mathrm{RCP}}$ is the difference between the diffusion coefficient of the RLP state and the RCP state, and α_0 is the maximum possible dilation as before.

Eq. (20) can be solved using a finite element method, such as the Crank–Nicholson procedure. In Fig. 10, we contrast our experimental results to the displacement of the tracers predicted by the diffusion–dilation model. The agreement is acceptable if the dilation coefficient is adjusted to $\alpha_0 \approx 0.1$ and can be further improved by adjusting D_{P} and α_0 simultaneously.

In Fig. 11, we compare the calculated displacement field including the dilation effect to previous dilation-less calculations. Whereas in the purely diffusive model (left panel) the displacement penetrates upward the entire cell, in the dilation model it progresses gradually from the bottom of the hopper (right panel). For further comparison each panel includes the IEZ and loosening body as well. In both cases, the maximum width of the IEZ varies as $W \sim \sqrt{D_{\mathrm{P}} H}$. Furthermore, at equal extracted volume, in the presence of dilation, the maximum width of the IEZ is slightly larger indicating that, at the lowest order, the presence of dilation is equivalent to a slightly larger diffusion coefficient. As recently summarized by Kuzmin [27], experimental evidence obtained in operating mines shows that the aspect ratio of the IEZ effectively obeys a diffusion type law for which $W \approx \sqrt{H}$. Our analysis shows, in addition, that the geometry of IEZ is not affected by dilation effects.

The aspect ratio of the motion zone can also be investigated. In the absence of dilation, the width of this zone increases linearly with the amount of extracted material [4]. In contrast, in the presence of dilation, this zone can be fitted by a power law as $W_1 \sim S^{0.5}$ which

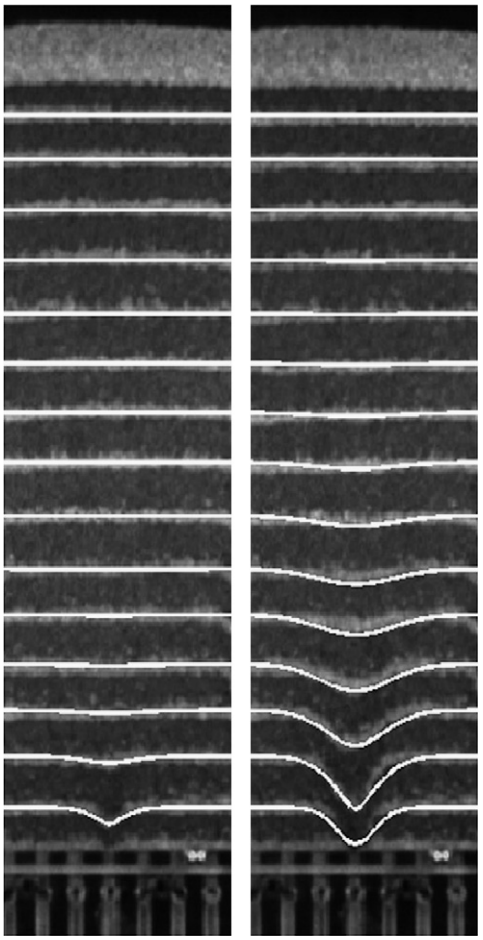

Fig. 10. Particles displacement from experimental visualization contrasted to the tracers displacement, as calculated from finite element procedure with a grid resolution of $\Delta x = d/4, \Delta y = d/8$, using the experimental parameter values and considering $\Delta D = 0$ and $\alpha_0 \approx 0.1$. The experimental parameters are $D_{\mathrm{P}} = d = 0.2\,\mathrm{cm}$, $v_0 = 2.2d$, $2D = 0.4\,\mathrm{cm}$ and $S = 4.5\,\mathrm{cm}^2$. (Left panel) Particles displacement calculations after one extraction. (Right panel) Particles displacement calculations after five extractions.

reproduces the behavior observed in our experiments [26]. However, calculations show that this power law might not be extended over a wide regime of draws and should be regarded with care.

Some interesting features of the evolution of the granulate free surface can be investigated with the help of the kinematic model. As the free surface moves with the grains, its vertical amplitude η obeys the partial differential equation,

$$\frac{\partial \eta}{\partial n} = v + u \frac{\partial \eta}{\partial x}, \qquad (21)$$

where n is the extraction step. Fig. 9 also shows the evolution of the free surface of the granulate. To solve Eq. (21), in a crude approximation, we assume that the displacement field is not affected by the presence of the free surface and it is sufficient to replace $v(\eta)$ and $u(\eta)$, obtained from relations (4) and (5), in Eq. (21) to determine the surface evolution. Since the granulate

Please cite this article as: Melo F, et al. Kinematic model for quasi static granular displacements in block caving: Dilatancy effects on drawbody.... Int J Rock Mech Mining Sci (2007), doi:10.1016/j.ijrmms.2007.07.005

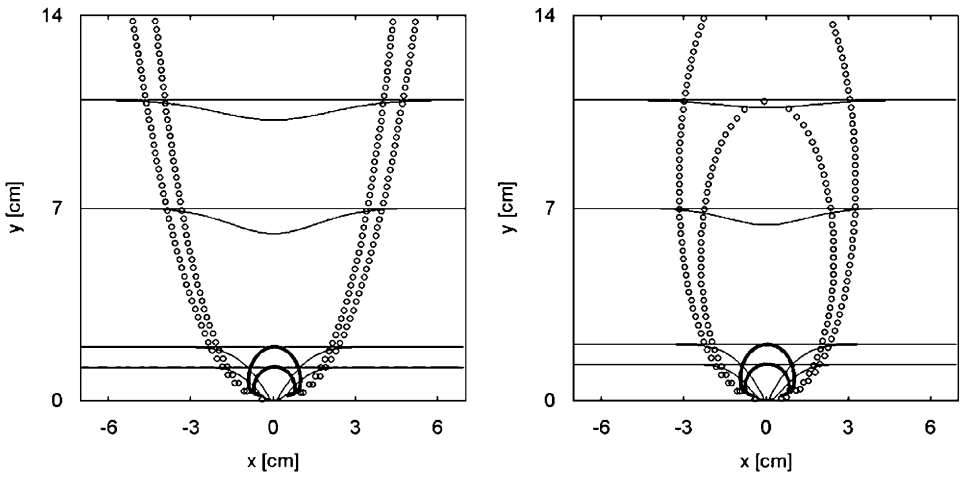

Fig. 11. Comparisons of tracers displacement, in the absence of dilation (left panel, $\alpha_0 = 0$), with dilation (right panel, $\alpha_0 = 0.1$), at several vertical levels after 0.8 extraction, as calculated from finite elements procedure with a grid resolution of $\Delta x = d/8, \Delta y = d/4$. In both panels, the diffusion coefficient is $D_P = d = 0.2\,\text{cm}$, $2R = 0.4\,\text{cm}$ and $v_0 = 2.2d$. Isolated extracted zones (solid lines) and loosening zones (open circles) are also displayed for 0.4 and 0.8 extractions.

dilation is not too high for the case depicted in the middle panel of Fig. 9, the kinematic model is able to capture reasonably well the evolution of the surface. For instance, at early stages of extraction, i.e., when $u(\eta)(\partial\eta/\partial x) \ll v(\eta)$ the surface deflection exhibits an inverted Gaussian shape which is consistent with a diffusive displacement field. However, for later stages of the extraction process, the granulate surface becomes more inclined and its dynamics dominated by intermittent or continuous avalanches that cannot be captured by the simple kinematic model, right panel of Fig. 9.

7.2. Discussion

Although the results presented above are deduced from rather simple situations compared to mining conditions, where heterogeneity of rocks, density changes, rocks shape and size reduction due to friction among others, play an important role, we believe that they might be useful for ore recovery optimization. For instance, recent experiments [16] have shown that no bulk segregation takes place in mixtures of granular materials that flow in hoppers. Significant size separation occurs only when the free surface becomes inclined at the avalanche angle. The mechanism of this effect is well known and a variety of situations can be found depending on the size contrast and particle shape, see [28]. Therefore, in granular mixtures, the kinematic model still can be applied if an effective diffusion coefficient is introduced. In addition, the information contained in the displacement field allows to determine the features of the maximum shear regions and should provide important insights about the particle size reduction due to this strong shear. Much experimental effort is, however, necessary to refine the simple description presented above to accurately describe complex flows encountered in actual mines.

7.3. Conclusions

Due to its linearity, the kinematic model is introduced to describe, in a first approximation, the granulate displacement field generated by an isolated hopper flow. When calculated and measured tracer movements are compared, by adjusting the diffusion coefficient to a value near to d, a good agreement is observed in regions close to the hopper aperture. However, due to the constant density assumption of the kinematic model in its original form, it cannot handle internal changes in volume taking place when the material starts to flow. This is reflected in the deviation of calculated positions of the tracers from the experimental ones, at distances far from the aperture. This discrepancy is corrected by considering the changes in local density through a dilation term. Then, at equal extracted amount of material, when dilation is present, a slightly larger maximum width is obtained which is equivalent to a slightly larger diffusion coefficient. Thus, the introduction of the dilation effect does not affect the functional dependence of height H with the width W and the relation $W \sim \sqrt{D_P H}$ still hold. In contrast, the loosening or motion zone is dramatically affected by dilation effects.

Experimental results show that neighboring hoppers interact notoriously when the distance between drawpoints is decreased. When high interaction occurs, which is also favored by the drawpoint width, the movement of the tracer particles located in the zone between drawpoints, resembles a constant descending flow with small lateral deformations. The main features of these interacting flows can be captured by considering the linear superposition of displacement fields produced by the individual drawpoints.

Thus, the development of the linear approximation as well as the "Diffusion–Dilatancy" equations provide a new tool to the study of more complex configurations, which might include stratified granular materials of different size

Please cite this article as: Melo F, et al. Kinematic model for quasi static granular displacements in block caving: Dilatancy effects on drawbody.... Int J Rock Mech Mining Sci (2007), doi:10.1016/j.ijrmms.2007.07.005

or even distinct packing as well as hoppers of more complex geometry. For instance, the generalization of these results to multiple hopper flows should not present any technical difficulty.

Acknowledgments

This work was supported by IM2 Codelco and Conicyt under research program Fondap no. 11980002.

References

[1] Laubscher, D. A practical manual on block caving, for the international caving study, 1997–2000.
[2] Brown, ET. Block caving geomechanics. The international caving study I, 1997–2000. JKMRC monograph series in mining and mineral processing, University of Queensland, vol. 3. Indooroopilly, Australia: JKMRC; 2003.
[3] Rustan, A. Gravity flow of broken rock—what is known and unknown. In: Conference proceeding of MassMin 2000: the Australasian institute of mining and metallurgy, 2000. p. 557–567.
[4] Melo F, Vivanco F, Fuentes C, Apablaza V. On drawbody shapes: from Bergmark–Roos to kinematic models. Int J Rock Mech Min Sci 2007;44:77–86.
[5] Kvapil R. Gravity flow of granular material in hoppers and bins, part 1. Int J Rock Mech Min Sci 1965;2:35–41.
[6] Kvapil R. Gravity flow of granular material in hoppers and bins, part 2. Int J Rock Mech Min Sci 1965;2:277–304.
[7] Janelid I, Kvapil R. Sublevel caving. Int J Rock Mech Min Sci 1966;3:129–53.
[8] Heslop TG, Laubscher DH. Draw control in caving operations on Southern African chrysotile asbestos mines. In: Stewart DR, editor. Design and operation of caving and sublevel stopping mines. New York: SME-AIME; 1981.
[9] Laubscher DH. Cave mining—the state of the art. J South African Inst Min Metall 1994;94:279–93.
[10] Laubscher, DH. Block cave manual, design topic: drawpoint spacing and draw control, Julius Kruttschnitt Mineral Research Centre, The University of Queensland, Brisbane, Australia; 2000.
[11] Marano, G. The interaction between adjoining draw points in free flowing materials and its application to mining. Chamber of Mines Journal, Zimbabwe; 1980. p 25–32.
[12] Janelid I. Study of the gravity flow process in sublevel caving. In: Proceedings of the international sublevel caving symposium. Stockholm: Atlas Copco; 1972.
[13] Peters, DC. Physical modeling of the draw behavior of broken rock in caving. Quarterly of the Colorado School of Mines, vol. 79(1), 1984.
[14] Power, GR. Modelling granular flow in caving mines: large scale physical modelling and full scale experiments. PhD thesis, The University of Queensland, Brisbane; 2004.
[15] Aranson IS, Tsimring LS. Patterns and collective behavior in granular media: theoretical concepts. Rev Mod Phys 2006;78:641–92.
[16] Samadani A, Pradham A, Kudrolli A. Size segregation of granular matter in silo discharges. Phys Rev E 1999;60:7203–9.
[17] Nedderman RM. Statics and kinematics of granular materials. Cambridge: Cambridge University Press; 1992.
[18] Bagnold RA. Experiment on a gravity-free dispersion of large solid spheres in a Newtonian fluid under shear. Proc R Soc London Ser A 1954;225:49–63.
[19] Beverloo WA, Leniger HA, van de Velde J. The flow of granular solids through orifices. Chem Eng Sci 1961;15:260–9.
[20] Behringer RP. The dynamics of flowing sand. Nonlinear Sci Today 1993;3:2–15.
[21] Mullins WW. Experimental evidence for the stochastic theory of particle flow under gravity. Powder Technol 1976;9:29–37.
[22] Litwiniszyn J. The model of a random walk of particles adopted to researches on problems of mechanics of granular. Bull Acad Pol Sci Ser Sci Technol 1963;9:61.
[23] Nedderman RM, Tüzün U. A kinematic model for the flow of granular material. Powder Technol 1979;22:243–53.
[24] Bransby PL, Blair-Fish PM. Initial deformations during mass flow from a bunker: Observation and idealizations. Powder Technol 1975;11:273–88;
Levinson M, Shmutter B. W. Resnick. Displacement and velocity fields in hoppers. Powder Technol 1977;16:29–43.
[25] Caram H, Hong DC. Random-walk approach to granular flows. Phys Rev Lett 1991;67:828–31.
[26] [a] Fuentes C, Apablaza V. Bi-dimensional experimentation on gravitational flow for underground chuquicamata. Internal report, IM2. Codelco-Chile 2003;
[b] Melo F, Vivanco F, Fuentes C, Apablaza V. Draft report on quasi static granular flows: dilatancy effects. Internal report IM2. Codelco-Chile 2005.
[27] Kuzmin YV. Forecast of the ore recovery in the bulk caving system. In: Proceedings Mass Min. Australia: Brisbane; 2000. p. 457–60.
[28] Duran J. Sables, poudres et grains. Paris: Eyrolles Sciences; 1997.

Please cite this article as: Melo F, et al. Kinematic model for quasi static granular displacements in block caving: Dilatancy effects on drawbody.... Int J Rock Mech Mining Sci (2007), doi:10.1016/j.ijrmms.2007.07.005